Reprinted from

International Journal of Applied Radiation and Isotopes, 1967, Vol. 18, pp. 835-847. Pergamon Press Ltd. Printed in Northern Ireland

Transmission through Aluminum of Beta-Particles Emitted by Infinitely-Thick Sources

R. H. RODRÍGUEZ-PASQUÉS, P. A. MULLEN,
G. A. GEORGE* and J. E. HARDING
National Bureau of Standards, Washington, D.C.

PERGAMON PRESS
OXFORD NEW YORK LONDON PARIS

International Journal of Applied Radiation and Isotopes, 1967, Vol. 18, pp. 835-847. Pergamon Press Ltd. Printed in Northern Ireland

Transmission through Aluminum of Beta-Particles Emitted by Infinitely-Thick Sources

R. H. RODRÍGUEZ-PASQUÉS, P. A. MULLEN,
G. A. GEORGE* and J. E. HARDING
National Bureau of Standards, Washington, D.C.

(*Accepted for publication* 31 *May* 1967)

The problem of determining the energy of beta-particles emitted from sources containing low concentrations of radioactive substances is examined. Transmission curves of beta particles emitted by "infinitely-thick" disc-shaped sources were obtained with two different detectors and compared to the curves similarly obtained for beta-particles coming from very thin "weightless" deposits on similar solid discs. Different matrix materials and beta-particle energies were used. The curves were studied for shape, secondary radiations and half-thickness. A series of curves were also obtained from four different potassium-salt thick sources, in order to investigate possible influences from variations of effective atomic number.

No substantial difference was found between the curves corresponding to the three types of sources, in connection with half-thickness-maximum-energy relationship.

Guiding rules are proposed for the determination of maximum beta-ray energies by means of absorption studies and half-thickness determination.

LA TRANSMISSION A TRAVERS L'ALUMINIUM DES PARTICULES BETA EMISES PAR UNE SOURCE D'EPAISSEUR INFINIE

On regarde le problème de mesurer l'énergie des particules béta émises par des sources qui contiennent de petites concentrations de matériaux radioactifs. On a obtenu des courbes de transmission des particules béta émises par des sources en forme de disques d'une "épaisseur infinie" avec deux détecteurs différents et on les a comparées aux courbes pareillement obtenues pour les particules béta sortant de dépôts très minces "sans poids" sur des disques solides et comparables. On a employé une variété de matériaux de matrice et une variété d'énergies de particules béta. On a étudié les courbes en rapport à la forme, aux rayonnements secondaires et à la demi-épaisseur. On a obtenu aussi une série de courbes de quatre différentes sources épaisses de sel de potassium, afin de poursuivre les influences possibles que pourrait donner une variation du nombre atomique effectif.

On ne trouva aucune différence signifiante entre les courbes qui correspondaient aux trois types de sources, en ce qui regarde le rapport de demi-épaisseur sur énergie maximum.

On propose des règles-guides pour la détermination des énergies maximum des rayons béta au moyen des études d'adsorption et de la mesure de la demi-épaisseur.

ПРОПУСКАНИЕ ЧЕРЕЗ АЛЮМИНИЙ ВЕТА-ЧАСТИЦ, ИЗЛУЧАЕМЫХ ИСТОЧНИКАМИ ВЕСКОНЕЧНОЙ ТОЛЩИНЫ

Изучается проблема определения энергии бета-частиц, излучаемых из источников, содержащих концентрацию радиоактивных веществ. Были получены кривые пропускания бета-частиц, излучаемых из дисковых источников "бесконечной толщины" при помощи двух различных детекторов. Эти кривые были сравнены с таким же образом полученными кривыми бета-частид, исходящих из очень тонких "невесомых" отложений. Употреблялись различные материалы матрид и энергии бета-частид. Кривые

* Present Address: Kerala University, Kerala, India.

изучались в отношении их формы, вторичного излучения и нолутолщины. Был также получен ряд кривых от четырех различных толстых источников солей калия для того, чтобы исследовать возможное влияние при изменении эффективного атомного номера.

Не было найдено значительной разницы между кривыми, соответствующими трем типам источников, в отношении между полутолщиной и максимальной энергией.

Предлагаются руководящие правила для определения максимальной энергии бета-лучей путем изучения поглощения и определения полутолщины.

DURCHGANG DURCH ALUMINIUM VON AUS UNENDLICH DICKEN QUELLEN EMITTIERTEN BETATEILCHEN

Es wird das Problem der Bestimmung der Energie von aus Quellen mit niedrigen Konzentrationen radioaktiver Substanzen emittierten Betateilchen untersucht. Es wurden Durchgangskurven von durch "unendlich dicken" Scheibenquellen emittierten Betateilchen mit zwei verschiedenen Detektoren erhalten und diese wurden mit ähnlichen Kurven für solche von sehr dünnen "gewichtlosen" Niederschlägen auf ähnlichen festen Scheiben verglichen. Verschiedene Matrixsubstanzen und Betateilchenenergien wurden verwendet. Die Kurven wurden auf Form, Sekundärstrahlung und HWS untersucht. Es wurde auch eine Serie von Kurven erhalten von vier verschiedenen dicken Kalisalzquellen, um etwaige Einflüsse durch Änderungen der reelen Atomzahl zu studieren.

Kein wesentlicher Unterschied wurde festgestellt zwischen den drei Quellentypen entsprechenden Kurven, hinsichtlich der Beziehung zwischen HWS und maximaler Energie.

Es werden Richtlinien vorgeschlagen für die Festlegung von maximalen Betastrahlenenergien durch Absorptionstudien und Bestimmung der HWS.

1. INTRODUCTION

THIS report is concerned with the identification of beta-particle emitters contained in certain materials having low-level radioactivity.

The problem of identifying pure beta-ray emitters is generally solved by determining their chemical identity, their half-life, and the maximum energy of the beta particles. Most frequently, the maximum energy is found by running a beta-ray absorption study and plotting the transmission versus the absorber thickness. From this plot, usually the range,[1–7] related to the maximum energy by well-known empirical expressions, is evaluated.[8,9] Alternatively, the half-thickness of the initial portions of the curves can be calculated and related to the maximum beta-particle energies.[10–12]

In the case of samples having low levels of radioactivity, it is either impossible or impractical to reach the maximum range, and this restricts the determination of beta-particle energies to the second alternative.

Low concentrations of radioactive substances make it advisable to prepare the sources by using as much sample mass as possible, in order to attain higher measuring efficiency. This means that thick extended sources will be preferred in such cases. This is different from the general procedure followed in transmission studies, where the trend is to prepare very thin, intense point sources. In view of this situation, it was thought desirable to conduct a research in order to gain a better knowledge of the peculiarities of the transmission curves resulting from such sources, and the appropriate way of using them as tools for the solution of the energy-determination problem.

A series of extended, thick, dense sources was prepared, and the corresponding transmission curves obtained. It was also thought of interest to compare them with the curves determined for a parallel series of sources consisting of very thin, surface layers of radioactive deposits, while keeping all other characteristics constant.

The curves were determined for various radionuclides (i.e. different beta-particle energies) and different source materials, and they were used for the evaluation of the corresponding half-thicknesses.

Complementary experiments were also carried out with a series of sources made of different potassium compounds (emitting nuclide: potassium-40), in order to investigate possible effects of variations of the effective atomic number of the source material on the resulting negatron transmission curve.

2. EXPERIMENTS

2.1 *Counters*

Two different commercial low-background detector instruments were used for the experiments. They will be called A and B.

Instrument A contains two counters within the same shell, in order to decrease the background rate by means of anticoincidence circuitry between both (Fig. 1). This double counter is heavily shielded by a lead castle. The detector belongs to the gas-flow type, working in the Geiger region; its aluminized "monomol resin" window has a thickness of about 150 $\mu g/cm^2$, and a dia. of 2 in. The counter is served by an automatic sample changer. During the counting of each source, the corresponding holder is raised close to the detector. A short distance, about half an inch, is kept between the bottom of the holder and the counter window, which was taken advantage of to run the absorption experiments.

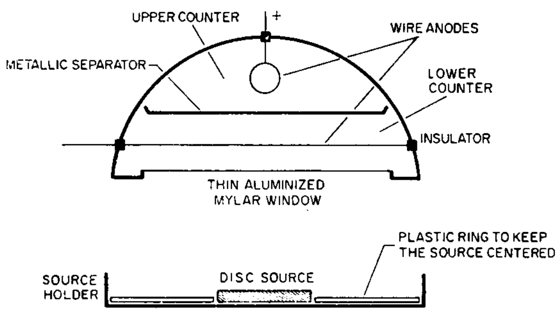

FIG. 1. Schematic drawing of window counter and source arrangement.

Instrument B presents similar features; it is not combined with an automatic changer.

The background rates of both instruments were about 45 counts per hr.

2.2 *Sources*

In all cases flat cylindrical source bodies were used, of 22·6 mm dia. and 3-mm thickness. Because of their shape, they will also be referred to as "discs". They are represented in Fig. 2, which also shows the distribution of radioactive material associated with these discs, constituting the sources proper. Two series of *thick* sources and one series of *thin* sources were prepared, as described in the following paragraphs.

2.2a *First series of thick sources*

The first series of thick sources was constituted by synthetic sources, made with pure substances purposely contaminated with small, known amounts of different added radioactively labelled substances. Table 1 gives the list of matrix components, their effective atomic number Z_{eff}, and their densities. Table 2 gives the radioactive additives used; the corresponding radioactive nuclides and some of their relevant properties are also indicated. Among them, the maximum ranges in aluminum are given, as found in the literature[9], and their equivalents in potassium salts, sulfur and iron, all in linear units. It can be seen that with one minor exception, none of these maximum ranges goes over 3 mm, the actual thickness of the source discs, which can thus be considered infinitely thick.

As already implied, the disc volume was constant, so that their actual mass varied according to the matrix used. The mass of

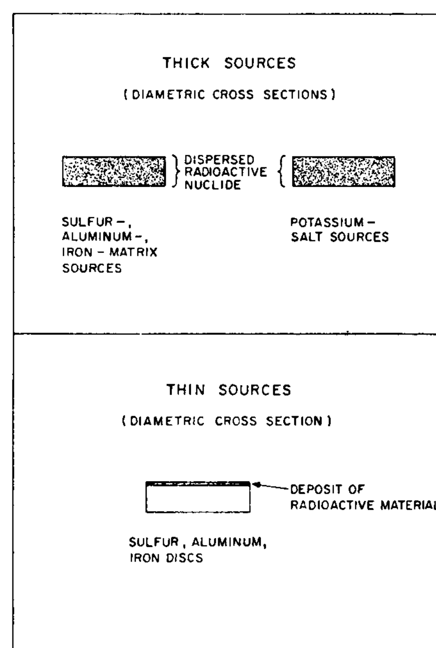

FIG. 2. Distribution of the radioactive nuclide in the different sources used.

TABLE 1

Series	Matrix substances	Densities of matrix substances*	Z_{eff}†
2.2a	Sulfur	2·07 g/cm³	16
	Aluminum	2·70 g/cm³	13
	Iron	7·86 g/cm³	26
2.2b	Potassium thiocyanate	1·89 g/cm³	14·7
	Potassium nitrite	1·92 g/cm³	12·9
	Potassium chloride	1·98 g/cm³	18·1
	Potassium chlorate	2·32 g/cm³	14·1

* Not density of actual sources. See text

† $Z_{eff} = \frac{\sum n_i A_i Z_i}{\sum n_i A_i}$

where n_i = number of atoms of class i in a molecule.

A_i = mass number of atoms of class i.

Z_i = atomic number of atoms of class i.

radioactive additive in each finished source was always kept at 20 mg.

Sulfur sources were prepared by melting sulfur in a small beaker, adding the radioactive substance in the appropriate amount and mixing by stirring with a glass rod. The mixture was poured into a nylon mold and left to cool slowly. It proved convenient to lubricate the internal mold surface previously with paraffin oil, in order to ease the removal of the disc. Since it was difficult to get a satisfactory distribution of the radioactive additive (as determined visually), only two different kinds of sulfur sources were prepared, containing either Ca^{45} or Sr^{89}. These discs were finished by gently grinding them down to size with sandpaper.

The aluminum and iron sources were prepared by thoroughly mixing the radioactive additives with aluminum or iron powders, respectively. The iron mixtures were then compressed to about 200,000 lb/in² and sintered at 1550°F into compact discs of approximately the density of iron. However, the iron mixture containing lead chloride was compressed but not sintered, in order to avoid loss of radioactivity due to the higher vapor pressure of the lead compound. The aluminum mixtures were likewise compressed but not sintered. The densities obtained for the mixtures were 99·3% that of pure aluminum and 94·9% that of pure iron respectively. Photomicrographs obtained during preliminary experiments with inactive additives showed the fine structure of such discs. The distribution of the additive inclusions between the metal granules depends largely on the nature of the additive and its physical properties. This is illustrated by the spreads of results when lots of similarly prepared radioactive sources were measured for counting rates. Table 3 gives an account of such data: there is a general parallelism of standard deviations for the corresponding aluminum and iron lots; Sr^{89}-containing sources are the most reproducible; S^{35} and Cl^{36} are the most variable lots, in both cases. The sources actually used for the absorption study were those having the counting rate closest to the average for the corresponding lot. Sometimes, a slight grinding of sharp rims was needed.

2.2b. *Second series of thick sources*

The second series of thick sources consisted entirely of discs prepared by melting potassium salts in a platinum crucible, pouring the melts into borosilicate glass molds, and grinding them down to size after solidification and cooling. Care was taken not to decompose the potassium chlorate by excessive heating. Potassium-40 was the radioactive nuclide in all these cases, and its distribution was, of course, perfectly homogeneous.

TABLE 2.

Labeled additives	Contained radionuclide	Half-life	Beta-particle maximum energy (MeV)	Maximum range in the different matrix materials* (mm)						
				Sulfur	Aluminum	Iron	Potassium thiocyanate KSCN	Potassium nitrite KNO_2	Potassium chloride KCl	Potassium chlorate $KClO_3$
Barium sulphate $BaSO_4$	S^{35}	87 days	0·167	—	0·12	0·041	—	—	—	—
Calcium carbonate $CaCO_3$	Ca^{45}	162·6 days	0·25	0·28	0·22	0·074	—	—	—	—
Lead chloride $PbCl_2$	Cl^{36}	3×10^5 yr	0·714	—	0·94	0·32	—	—	—	—
Strontium carbonate $SrCO_3$	Sr^{89}	50·7 days	1·46	3·13	2·41	0·83	—	—	—	—
Magnesium pyrophosphate $Mg_2P_2O_7$	P^{32}	14·3 days	1·71	—	2·89	0·99	—	—	—	—
Potassium salts	K^{40}	$1·27 \times 10^9$ yr	1·32†	—	—	—	2·99	2·94	2·85	2·43

* Calculated from the ranges in aluminum.
† Also emits conversion electrons (γ-ray energy: 1·46 MeV).

TABLE 3

Source Matrix/emitter	Number of sources counted	Average counting rate per unit weight (cpm/g)	σ (cpm/g)	σ%
Al/S^{35}	6	916·1	50·3	5·5
Al/Ca^{45}	6	1606·0	12·4	0·77
Al/Cl^{36}	6	424·1	52·3	12·3
Al/Sr^{89}	6	300··4	0·75	0·25
Al/P^{32}	6	95·4	1·81	1·9
Fe/S^{35}	6	624·7	78·3	12·5
Fe/Ca^{45}	6	250·2	11·1	4·4
Fe/Cl^{36}	6	89·6	7·8	8·7
Fe/Sr^{89}	5	39·4	0·37	0·94
Fe/P^{32}	6	19·0	0·64	3·4

2.2c. *Series of thin sources*

A series of *thin*, weightless sources was also prepared, for comparison purposes, by evaporating radioactive solutions, of very low solid content, spread on top of inactive, 3-mm thick synthetic aluminum and iron discs, entirely similar to the thick radioactive source bodies described in Section 2.2a above. The resulting deposits were "cleaned" by gently rubbing with wet paper "tissue", and further drying. This assured that only an adsorbed, weightless layer of radioactive substance remained on top of each 3-mm backscatterer disc.

2.3. *Absorbers—Technique*

The absorbers were plain aluminum discs, 2 in. in dia., mounted on thin ring-shaped narrow bakelite frames.

The sources were placed in the counter holders (i.d. 2 in.) and kept centered by means of ring-shaped flat lucite pieces (Fig. 1). Counts were taken for as long as practically possible, so as to obtain good counting statistics. Statistical counting errors naturally increase when the total number of counts is diminished by thicker absorbers. For the three lower-energy beta-particle emitters used (S^{35}, Ca^{45}, Cl^{36}), the relative standard deviations, RSD, of all points within at least the first four half-thicknesses were kept below 3%, except in one case (Ca^{45} in the thick sulfur matrix, Fig. 3, for which the RSD increased to about 5% at 2·5 half-thicknesses).

For the higher-energy beta-particle emitters (K^{40}, Sr^{89}, P^{32}), it was possible to maintain the RSD under 3% for all points within at least the first half-thickness, except in two cases (Sr^{89} in

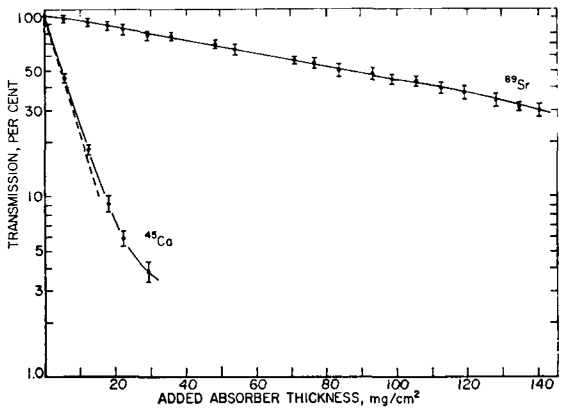

FIG. 3. Transmission curves for beta-particles emitted by the indicated radionuclides contained in thick sulfur matrices—Detector A.

the thick sulfur matrix, Fig. 3, and P^{32} in the thick iron matrix, Fig. 6, for which the RSD was already about 3% at 2/3 half-thickness).

For a definite majority of the points determined, the RSD was 1% or better. Although points with statistics poorer than the above-stated limits have been represented in the graphs, no decisive weight was given to them, individually, in setting the direction of the transmission curves. No transmissions were determined beyond 150 mg/cm^2 of added absorber thickness.

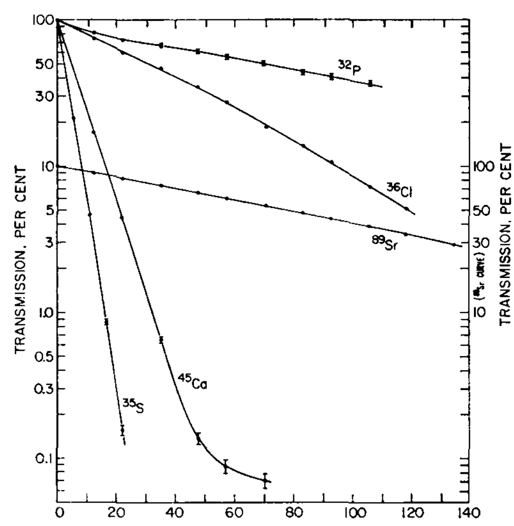

FIG. 4. Transmission curves for beta-particles emitted by the indicated radionuclides, contained in thick aluminum matrices—Detector A.

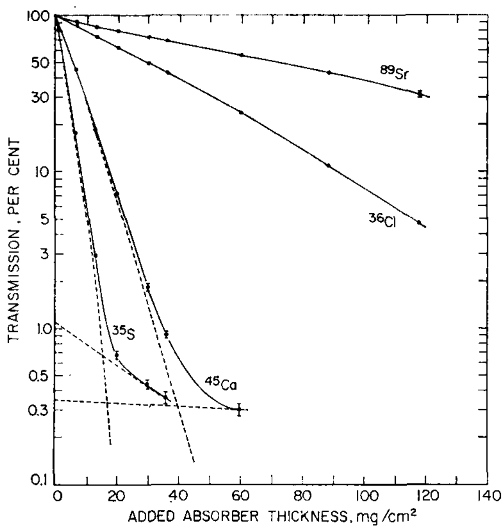

FIG. 5. Transmission curves for beta-particles emitted by the indicated radionuclides contained in thick aluminum matrices—Detector B.

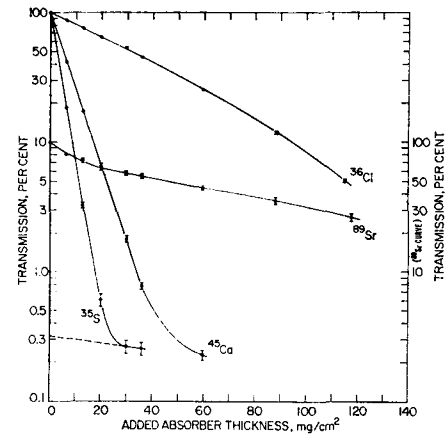

FIG. 7. Transmission curves for beta particles emitted by the indicated radionuclides contained in thick iron matrices—Detector B.

3. RESULTS

Figures 3–7 show the transmission curves obtained for thick synthetic sources, normalized to 100% for the initial point, corresponding to zero added absorber thickness, in each case. Figures 8–11 represent the parallel series of transmission curves for thin sources, and Fig. 12 shows the curves for potassium salt sources, all normalized in the same way.

In a first approximation, all the curves are exponential, but they also present peculiarities which are discussed in the next paragraphs.

A very soft, low-intensity component, constituted by backscattered particles, appears superimposed on most of the absorption curves for the more energetic beta radiations. From the graphs, it appears that this soft component is more intense when the atomic number of the scatterer is higher, as repeatedly observed

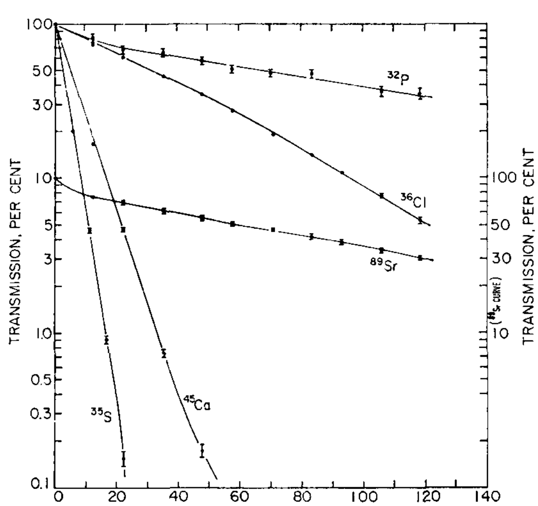

FIG. 6. Transmission curves for beta-particles emitted by the indicated radionuclides contained in thick iron matrices—Detector A.

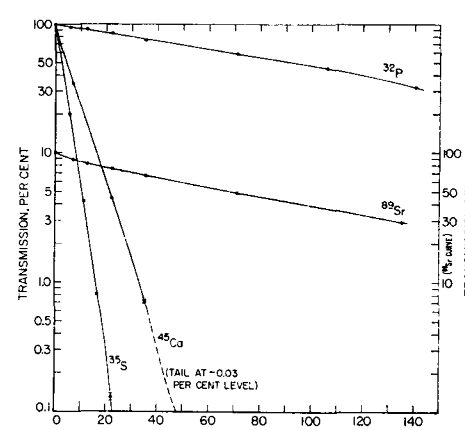

FIG. 8. Transmission curves for beta particles emitted by the indicated radionuclides spread in a thin layer on top of aluminum discs—Detector A.

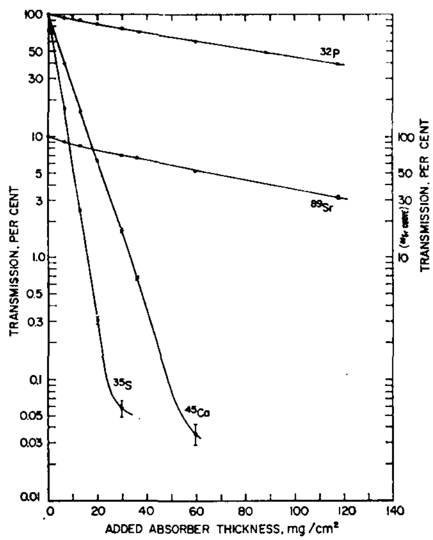

FIG. 9. Transmission curves for beta-particles emitted by the indicated radionuclides spread in a thin layer on top of aluminum discs—Detector B.

before.[4,10] Backscattering effects occur independently of source thickness in the discs.

Tails due to hard components were detected when the sources were thick and the beta rays soft enough for the maximum range to be overrun, i.e. S^{35} and Ca^{45}. Since these are pure beta-emitters, the tails must be considered a *bremsstrahlung* effect. The tails are frequently too low in intensity to warrant any correction

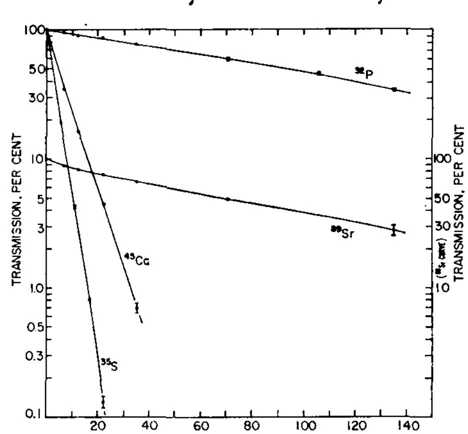

FIG. 10. Transmission curves for beta-particles emitted by the indicated radionuclides, spread in a thin layer on top of iron discs—Detector A.

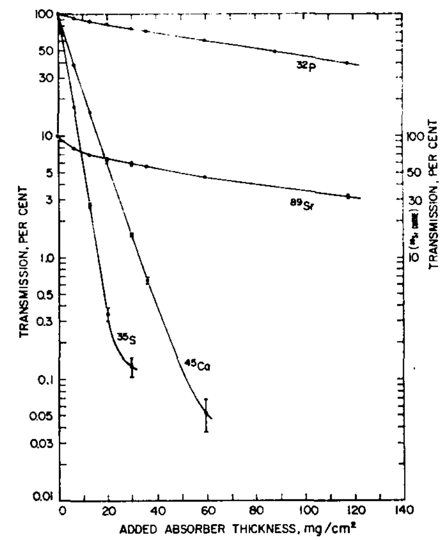

FIG. 11. Transmission curves for beta-particles emitted by the indicated radionuclides, spread in a thin layer on top of iron discs—Detector B.

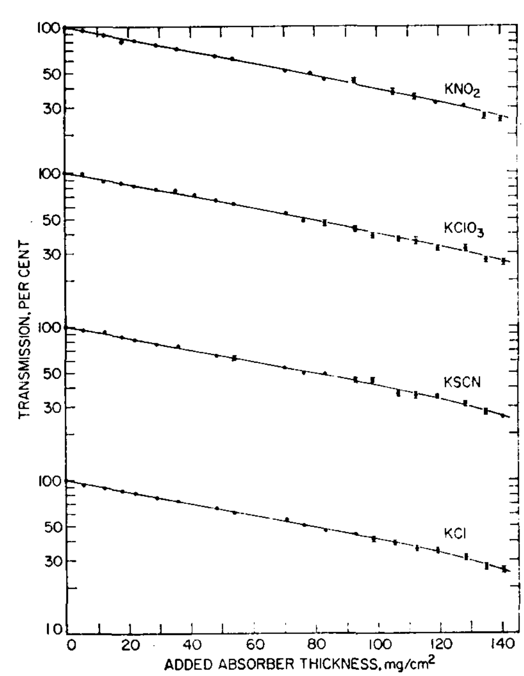

FIG. 12. Transmission curves of negatrons emitted by different thick potassium-salt sources—Detector A.

of the transmission curves by subtracting their contribution; the effect is therefore ignored when the extrapolated tails intersect the ordinate axis below 0·35 %, for the reasons explained at the end of this Section.

Potassium-40 is not a pure beta-emitter: negatron emission occurs in 89 % of the decays, and electron capture in the remaining 11 %, to an excited state of argon-40; since the subsequent single gamma-ray (1·46 MeV) is highly converted ($CE/\gamma \simeq 1$), monoenergetic electrons are also emitted in 5·5 % of the decays[13]. The photon intensity is therefore low; for the conditions of this study, it was found that the ratio of counted photons to electron particles was, at the most, 1:225, thus making any correction of the curves for the calculation of half-thicknesses unnecessary.

The calculation of the half-thicknesses $d_{1/2}$ is based on the well known equation,

$$R = R_0 \, . \exp\left(-0{\cdot}693 \frac{d}{d_{1/2}}\right), \qquad (1)$$

where R = counting rate when the absorber thickness is d.

R_0 = counting rate when no absorber is interposed.

From this, the practical expression is obtained:

$$d_{1/2} = \frac{0{\cdot}3009(d_2 - d_1)}{\log R_1 - \log R_2}. \qquad (2)$$

R_1 and R_2 are any two counting rates for the particles transmitted through absorber thicknesses d_1 and d_2, respectively, conveniently taken from a truly exponential section of the transmission curve.

In connection with this calculation, it is convenient to divide the transmission curves plotted in Figs. 3–11 into two groups: (1) "soft curves", corresponding to S^{35}, Ca^{45} and Cl^{36}, and (2) "hard curves", for Sr^{89} and P^{32}. The *soft* curves do not present marked scattering effects, although some of the initial sections do show slight "irregularities"; because these are very small, they have been ignored, and the curves are considered truly exponential at their beginning. Due to clear scattering effects, the initial parts of the *hard* curves, up to about 30 mg/cm^2 are generally not exponential. On the other hand, these curves begin to bend downwards after about 60 mg/cm^2, so that only the intermediate "central" sections can be considered truly exponential; it is from these central sections that the half-thickness values for the hard curves were computed. In spite of their corresponding hard energy, the curves for K^{40} present initial sections exponential, but this is probably accounted for by the low density of the matrix potassium salts, giving rise to negligible scattered-particle intensity.

The calculated half-thicknesses are given in Table 4. Some considerations about their precision are in order. As shown in Appendix A, it is easy to find that

$$\frac{\Delta d}{d_{1/2}} = \frac{\log (1 + \Delta R/R)}{2 - \log (R + \Delta R)} \qquad (3)$$

where $\Delta d/d_{1/2}$ is the relative error in the half-thickness when the direction of the exponential curve changes in such a way that the transmission at $d_{1/2}$ varies from R to $R + \Delta R$. In other words, $\Delta R/R$ is the corresponding relative variation in counting rate in the vicinity of the half-thickness value.

As explained at the end of Section 2, the standard deviations of the experimentally determined counting rates within the exponential sections of the curves actually used for calculations, were generally below 3 %, to which corresponds a "95 % confidence level error" of 6 %. Using this upper value for $\Delta R/R$, and giving R its numerical value of 50, the calculation gives $\Delta d/d_{1/2} = 0{\cdot}09$; in other words, the upper limit of error to be expected at 95 % confidence level, from purely statistical counting variations, is 9 %. Absorber counting-rate blank (background) determination errors should also be included, but their contribution within the "linear" ranges of the curves, is very low, due to the smallness of the blank rates themselves: they ranged between 0·6 and 2·0 cpm in *all* cases, a large majority of values being less than 1 cpm. Blank count rates were determined with the absorbers in position, to allow for radioactivity or scattering in the absorbers themselves.

Additional sources of errors are: Uncertainty in the absorber thickness, geometry variations, neglecting to substract *bremsstrahlung* contribution, and defects in drawing the graphs. The

TABLE 4(a). Thin weightless radioactive sources on 3-mm-thick backscatterers

Counter	B		A	
Back-scatterer	Al (mg/cm²)	Fe (mg/cm²)	Al (mg/cm²)	Fe (mg/cm²)
Radio-nuclides				
S^{35}	2·5	2·5	2·4	2·5
Ca^{45}	5·1	5·0	5·1	5·1
Sr^{89}	73	75	80	77
P^{32}	90	89	92	95

first two can be considered negligible; in connection with the latter, special care has been exercised to keep consistency and to avoid any bias; this was helped by representing the 2σ limit of all experimental points by vertical segments, and using these as guides for setting the proper course direction of each curve. Only those segments corresponding to relative σ's larger than 3% are shown on the illustrations. As already stated, tails were not subtracted when their contribution was 0·35%, or less; this particular value was chosen because it determines a 1% error on the calculation of $d_{1/2}$ (Appendix B).

TABLE 4(b). 3-mm-thick radioactive source discs

Counter	B		A						
Matrix	Al (mg/cm²)	Fe (mg/cm²)	sulfur (mg/cm²)	Al (mg/cm²)	Fe (mg/cm²)	KNO_2 (mg/cm²)	$KClO_3$ (mg/cm²)	KSCN (mg/cm²)	KCl (mg/cm²)
Radio-nuclides									
S^{35}	2·5	2·6	—	2·5	2·5	—	—	—	—
Ca^{45}	4·9	5·1	4·9	4·9	5·1	—	—	—	—
Cl^{36}	30	32	—	31	32	—	—	—	—
Sr^{89}	78	78	80	77	79	—	—	—	—
P^{32}	—	—	—	90	93	—	—	—	—
K^{40}	—	—	—	—	—	76	78	78	79

TABLE 5.

	Half-thicknesses		
	This work		
β-Ray maximum energies (MeV)	Pooled values (mg/cm²)	RSD* of pooled values (%)	From D. W. ENGELKEMEIR's curve (NNES IV, 9, Book 1, p. 18) mg/cm²
0·167	2·5	2·2	3·0
0·25	5·0	2·0	5·0
0·714	31·0	3·1	26·0
1·46	77·5	3·1	63·0
1·71	91·0	2·5	81·0

* RSD = relative standard deviation.

4. CONCLUSIONS

The calculated half-thicknesses (Table 4) are remarkably independent of radioactive source thickness, matrix material or even detector used. The reason for the latter must be attributed to the coincidental similarity between the instruments chosen; in fact, the half-thickness values found by other researchers, who used a differently shaped end-window Geiger-Müller counter *are* different, although not greatly so, from the values found during the present study.[10–12] As an illustration, there are given in Table 5 averaged values obtained from Table 4, and the corresponding ones as taken from the graph of ENGELKEMEIR.[10, pp. 18–19]

Except for the secondary effects already described, the transmission curves for infinitely thick sources and for thin weightless sources on thick backscatterers are similar. According to this, no significant error should be expected in the determination of $d_{1/2}$ when the source thickness is smaller than the maximum range of the emitted particles in the matrix material.

No noticeable effect was observed which could be attributed to variations of effective atomic number of source material.

With regard to the purpose of beta-ray-energy determination, consideration must be given to serious uncertainty in the values of $d_{1/2}$ that can arise from backscattering effects, unless precautions are taken to select an appropriate exponential section of the curves, as was done for the calculations presented in this report. These can be condensed in the following guide lines:

(1) Determine several transmission points for absorber thicknesses between 0 and 30 mg/cm^2.

(a) When the radiation is soft, all of the exponential curve will probably be contained within this range. $d_{1/2}$ is calculated from the exponential curve.

(b) If the beta-particles are energetic, a curvature due to scattered radiation will probably appear in this section.

(2) In the case of (1)(b) above, it will be necessary to determine points for the 30–60 mg/cm^2 thickness range. These will include the exponential section, from which $d_{1/2}$ can be adequately evaluated.

(3) In the case of soft beta-particles emitted from low-intensity matrices (organic substances, plastics) it might be necessary to correct for the presence of comparatively intense *bremsstrahlung*; in consequence, enough absorber thicknesses should be used, in this case, so as to reveal the tail and evaluate its contribution.

(4) When dealing with radionuclide *mixtures*, a study of the shape of the initial, central and final sections of the corresponding curve should help to a possible resolution of the component transmission curves.

Once $d_{1/2}$ is calculated, the maximum beta-particle energy can be obtained directly from the graph presented in Fig. 13, for which the half-thicknesses for different kinds of instruments and sources have been pooled into single values, as in Table 5, and have been represented vs. the corresponding beta-particle maximum energies. A logarithmic plot, where segments representing uniform errors keep constant lengths, has been preferred.

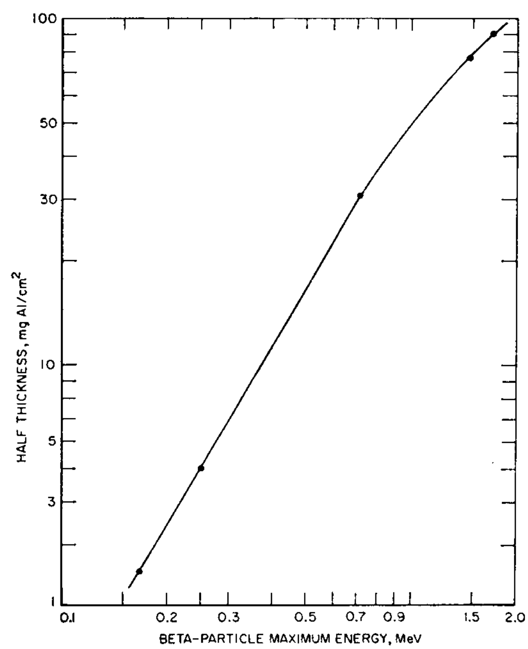

FIG. 13. Pooled half-thickness values as a function of beta-particle maximum energies.

Acknowledgements—The authors wish to express their appreciation to Dr. M. R. MEYERSON and Mr. T. P. ROYSTON, of the Metallurgy Division, National Bureau of Standards, and to the International Powder Metallurgy Company, of Ridgeway, Pennsylvania, for their competent help in preparing the synthetic iron and aluminum thick-source discs.

Partial financial support was provided by the Division of Research, U.S. Atomic Energy Commission.

REFERENCES

1. Feather N. *Proc. Cambridge Phil. Soc.* **34,** 599 (1938).
2. Bleuler E. and Zünti W. *Helv. Phys. Acta* **19,** 375 (1946).
3. Glendenin L. E. *Nucleonics* **2,** 12 (1948).
4. Zumwalt L. R. Absolute beta-counting using end-window Geiger-Müller counters and experimental data on beta-particle scattering effects. U.S. Atomic Energy Commission Report AECU-567 (1950).
5. Katz L. and Penfold A. S. *Rev. Mod. Phys.* **24,** 28 (1952).
6. Harley J. H. and Hallden N. A. *Nucleonics* **13,** 32 (1955).
7. Barreira F. and Laranjeira M. *Int. J. appl. Radiat. Isotopes* **2,** 145 (1957).
8. Overman R. T. and Clark H. M. *Radioisotope Techniques*, p. 217. McGraw-Hill (1960).
9. Friedlander G., Kennedy J. W. and Miller J. M. *Nuclear and Radiochemistry*, pp. 106–107. Wiley (1964).
10. Coryell C. D. and Sugarman N. (editors) *Radiochemical Studies: The Fission Products*, National Nuclear Energy Section, Division IV, Vol. 9, Book 1, Part I (1951).
11. Pappas A. C. A radiochemical study of fission yields . . . , p. 41. U.S. Atomic Energy Commission Report AECU-2806 (1953).
12. *Radiological Health Handbook*, p. 135. U.S. Department of Health, Education and Welfare (1960).
13. National Academy of Sciences–National Research Council. *Nuclear Data Sheets*, current sheet for atomic number 40.

APPENDIX A

Calculation of theoretical error of half-thickness value

In Fig. 14, triangles $\overset{\triangle}{ABC}$ and $\overset{\triangle}{MNC}$ are similar; then:

$$\frac{\Delta \log R}{\Delta d} = \frac{\log R_0 - \log R}{d + \Delta d} \qquad (1)$$

Rearranging:

$$\frac{d + \Delta d}{\Delta d} = \frac{\log R_0 - \log R}{\Delta \log R} = \frac{\log R_0 - \log R}{\log (R + \Delta R) - \log R} \qquad (2)$$

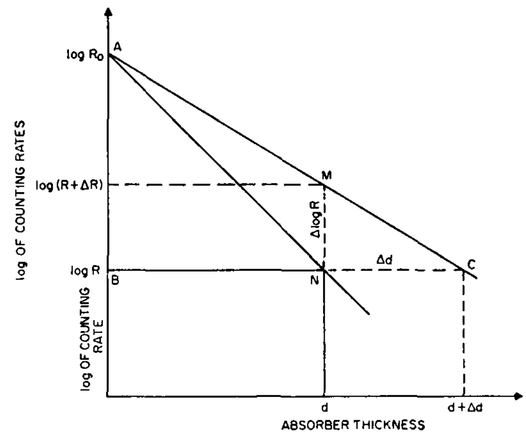

Fig. 14. Variation of half-thickness with direction of transmission curve.

$$\frac{d}{\Delta d} = \frac{\log R_0 - \log R}{\log (R + \Delta R) - \log R} - 1 \qquad (3)$$

$$\frac{d}{\Delta d} = \frac{\log R_0 - \log R - \log (R + \Delta R) + \log R}{\log (R + \Delta R) - \log R} \qquad (4)$$

Simplifying and inverting:

$$\frac{\Delta d}{d} = \frac{\log (R + \Delta R)/R}{\log R_0 - \log (R + \Delta R)} = \frac{\log (1 + \Delta R/R)}{\log R_0 - \log (R + \Delta R)} \qquad (5)$$

Since $R_0 = 100$, we can write, for $d = d_{1/2}$:

$$\frac{\Delta d}{d_{1/2}} = \frac{\log \left(1 + \frac{\Delta R}{R}\right)}{2 - \log (R + \Delta R)}$$

APPENDIX B

"Tail" subtraction

It is desired to find out the subtracted tail value, t, which would cause a 1% variation in the value of $d_{1/2}$. In this general form, this is an indeterminate problem, because the shift in $d_{1/2}$ will also depend on the half-thickness of the tail. By definition, however, the tail decreases slowly and no serious error will be introduced if the tail value, t, is assumed to be constant.

Figure 15 shows that in the vicinity of the half-thickness, $d_{1/2}$, a decrease of the per cent

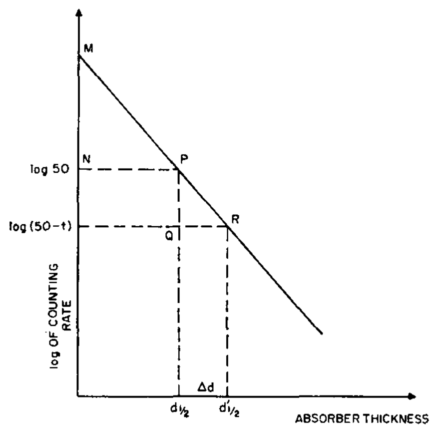

FIG. 15. Variation of half-thickness with subtraction of *bremsstrahlung* tail.

transmission from 50 to 50 − t causes a shift Δd of the half-thickness, to the new value $d'_{1/2}$. Since triangles $\overset{\Delta}{\mathrm{MNP}}$ and $\overset{\Delta}{\mathrm{PQR}}$ are similar, it is possible to state that

$$\frac{\log 50 - \log (50 - t)}{\Delta d} = \frac{\log 100 - \log 50}{d'_{1/2}}$$

Multiplying by −1 and reordering

$$\frac{\Delta d}{d'_{1/2}} = \frac{\log (50 - t) - \log 50}{\log 50 - \log 100}$$

But

$$\frac{\Delta d}{d'_{1/2}} \cong \frac{\Delta d}{d_{1/2}} \equiv 0{\cdot}01, \text{ so that}$$

$$\log (50 - t) = 0{\cdot}01 (\log 50 - \log 100) + \log 50$$

Then

$$t = 0{\cdot}35$$